XVIII. COMMUNICATIONS BIOPHYSICS*

Academic and Research Staff

Prof. S. K. Burns
Prof. P. R. Gray†
Prof. R. W. Henry‡
Prof. P. G. Katona
Prof. N. P. Moray**
Prof. W. T. Peake††
Prof. W. A. Rosenblith
Prof. W. M. Siebert
Prof. T. F. Weiss††
Prof. M. L. Wiederhold††
Dr. J. S. Barlow‡‡
Dr. G. O. Barnett***
Dr. A. Borbely†††
N. I. Durlach
Dr. O. Franzen‡‡‡
Dr. R. D. Hall
Dr. N. Y. S. Kiang††
Dr. M. Nomoto****
Dr. K. Offenloch†††††
R. M. Brown††
A. H. Crist††
F. N. Jordan
W. F. Kelley
E. G. Merrill

Graduate Students

T. Baer
J. E. Berliner
L. D. Braida
R. C. Cerrato
H. S. Colburn
L. A. Danisch
P. Demko, Jr.
J. J. Guinan, Jr.
Z. Hasan
A. Houtsma
E. C. Moxon
N. M. Nanita
R. E. Olsen
R. E. Peterson
P. L. Poehler
D. J-M. Poussart
A. V. Reed
R. S. Stephenson
A. P. Tripp
B. A. Twickler
D. R. Wolfe

---

*This work was supported principally by the National Institutes of Health (Grant 1 PO1 GM-14940-01), and in part by the Joint Services Electronics Programs (U.S. Army, U.S. Navy, and U.S. Air Force) under Contract DA 28-043-AMC-02536(E), the National Aeronautics and Space Administration (Grant NsG-496), and the National Institutes of Health (Grant 1 TO1 GM-01555-01).

†Leave of absence, at General Atronics Corporation, Philadelphia, Pennsylvania.

‡Visiting Associate Professor from the Department of Physics, Union College, Schenectady, New York.

**Visiting Associate Professor from the Department of Psychology, University of Sheffield, Sheffield, England.

††Also at the Eaton-Peabody Laboratory, Massachusetts Eye and Ear Infirmary, Boston, Massachusetts.

‡‡Research Affiliate in Communication Sciences from the Neurophysiological Laboratory of the Neurology Service of the Massachusetts General Hospital, Boston, Massachusetts.

***Associate in Medicine, Department of Medicine, Harvard Medical School, and Director, Laboratory of Computer Science, Massachusetts General Hospital.

†††Postdoctoral Fellow from the Brain Research Institute, University of Zurich, Zurich, Switzerland.

‡‡‡Postdoctoral Fellow from the Speech Transmission Laboratory, The Royal Institute of Technology, Stockholm, Sweden.

****Public Health Service International Postdoctoral Research Fellow, from the Department of Physiology, Tokyo Medical and Dental University, Tokyo, Japan.

†††††Postdoctoral Fellow from the Max Planck Institut for Brain Research, Frankfurt, Germany.

A. SOUND-PRESSURE TRANSFORMATION BY THE EXTERNAL EAR OF THE CAT

In a study on the acoustic properties of the cat's external ear, the sound-pressure transformation from a free-sound field to the eardrum has been measured. In behavioral auditory threshold determinations the stimulus is often specified in terms of free-field sound pressure, whereas measurements of middle-ear transmission and threshold responses of auditory-nerve fibers are usually referred to the sound pressure at the eardrum. The sound-pressure transformation data may be used to relate these two groups of measurements.

Amplitude and phase of the sound-pressure transformation have been measured up to 15 kHz for several experimental conditions, such as opened or closed bulla and various sound-source azimuths.

In an attempt to investigate the physical factors that limit the sound-source localization process in the cat, interaural sound pressure ratios and phase differences have been determined for various sound-source azimuths.

G. von Bismarck, R. R. Pfeiffer

B. INVESTIGATIONS ON THE ABDOMINAL STRETCH RECEPTOR SYSTEM OF CRAYFISH

The crayfish, a miniature freshwater version of the lobster, has an interesting network of proprioceptors in its segmented tail.[1] Each side of each of the 6 abdominal segments contains a pair of stretch receptor organs. Each receptor organ is connected with the cell body of an afferent neuron in such a way that when the tail is flexed, thereby increasing the length of the receptor organ, the receptor neuron responds with a train of nerve impulses which are transmitted directly to the central nerve cord of the animal. One of each pair of stretch receptor organs apparently sends information about the amount of flexion between adjacent segments, for its neuron fires at a quite constant frequency for a constant amount of flexion. The other organ of the pair apparently sends information that a sudden increase in flexion has occurrred, for its neuron fires only in response to a large, quickly applied flexion and stops firing within a few seconds.

While the details of the way in which mechanical stress in the receptor organ elicit an action potential on the receptor neuron have received considerable attention only R. O. Eckert has studied the entire network of (24) stretch receptors.[2] Eckert's main finding was that when the firing rate of a receptor neuron in one segment is increased (by deforming the receptor organ) to 50-100 impulses/sec, efferent pulse trains are elicited in nearby (especially the adjacent) segments. An efferent pulse train was observed to cause a drastic reduction of the firing rate of the receptor neuron in that segment. Eckert's work and some anatomical evidence suggest that there is a single

efferent inhibitor neuron which synapses with, and can modulate the firing rate of, both of the receptor neurons on one side of one segment.

In all of the previous work, including Eckert's, the surgery involved considerable loss of blood and rather rapid (1-3 hours) deterioration of the preparation and death of the animal. To counteract the loss of blood and delay deterioration, the preparation is always bathed in physiological saline solution. It has been found,[3] however, that a crustacean's utilization of oxygen can be seriously reduced when the fluid bathing its breathing apparatus is excessively salty. Hence, the condition of the animal and, in particular, of the central nervous system, which must receive oxygen from the circulatory system and not the bathing medium, must be suspect in the aforementioned experiments.

Recently our group has developed a very simple technique for recording from the dorsal nerve bundle (which includes the stretch receptor neurons) which (a) does not result in death of the animal, and (b) allows the animal relatively complete freedom of movement. The method employs fine wire electrodes anchored to the shell of several segments. The end of an electrode wire makes contact with the body fluid near the dorsal nerve bundle through a small hole drilled in the shell, and can record nerve impulses on several of the half dozen or so nerve fibers in the bundle, as well as electrical activity in the extensor muscles. When two such wires are used (one distal and the other proximal) on one side of one segment, one receives unambiguous information about the direction of travel (afferent or efferent) of the impulse and its velocity. Relative velocity measurements are an excellent way of identifying nerve spikes on different fibers, since the relative velocity does not depend on the precise position of the electrode relative to the nerve, as would, for example, relative amplitude measurements. The advantages of our in vivo recording methods are the following.

1. There can be no deterioration of the nervous system, because of loss of blood or lack of oxygen.

2. Stretch receptor activity (and activity in other neurons in the dorsal bundle and in the extensor muscles) can be investigated over a long period of time, so that variations caused by interactions of the stretch receptor system with other subsystems of the nervous system can be observed and studied. (The first animal used in the development of these techniques lived through two weeks of experimentation.)

3. Study of the stretch receptor activity can be made with the animal in normal postures, as well as in artificially induced abnormal postures.

4. Stretch receptor activity can be observed during active flexion or extension, since the electrodes remain in position even during violent motion.

The present experiments involve both a further study of the stretch receptor system itself, including the mutual inhibition observed by Eckert, and the elucidation of the role that the stretch receptor system plays in the over-all nervous system of the animal. Although this is primarily a progress report, several preliminary results are

worth pointing out.

1. Considerable flexion is required in order for receptor neurons to fire at all. In the animal's normal resting positions, even with the tail tucked beneath the body in a position of extreme flexion, the stretch receptor firing rates tend not to be as high as the 50-100 spikes/sec rate Eckert used to observe inhibitory effects in adjacent segments.

2. On the other hand, we have observed an inhibitory effect on the stretch receptor neurons in response to rather general mechanical stimulation of hairs on the skeleton; for example, hairs on the uropods (tail fins) and at the back of the carapace (thoracic shell). Such mechanical stimulation gives rise to a short-lived (1-5 sec) burst of efferents on the dorsal nerve bundles and a significant (up to 50%) decrease in the average receptor neuron firing rate while the efferent burst lasts.

3. Under certain conditions, a single stretch receptor nerve spike elicits a spike on a motor nerve which drives the superficial extensor muscles in the same segment. Often both the brief motor-nerve spike and the associated long-lasting electrical muscle activity can be observed at the same time. The delay between the afferent receptor spike and the efferent motor spike or resultant muscle activity is quite constant (approximately 20 msec) and consistent with the travel times for the nerve spikes to and from the central nervous system. Figure XVIII-1 shows the average of several hundred responses to an afferent stretch receptor nerve spike. The data were recorded on ARC, an average response computer.

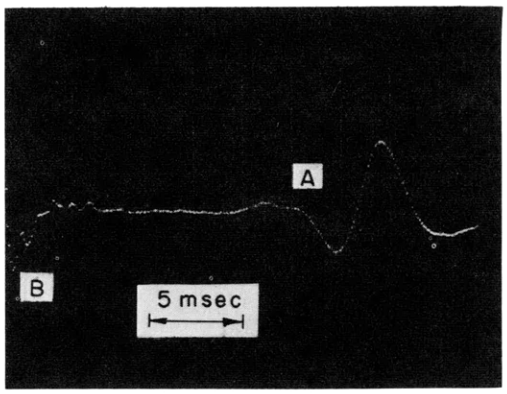

Fig. XVIII-1. The average of several hundred responses to a stretch receptor nerve impulse, as recorded on a distal electrode. Zero time represents the arrival of a nerve impulse at a proximal electrode. The slow wave at A is the muscle activity. The negative slope at the extreme left is the trailing edge of a positive-going stretch receptor impulse whose leading edge has already passed the recording electrode. The positive deflections near B represent impulses on efferent neurons whose arrival at the proximal electrode triggered the average response computer.

The relation between the apparent inhibition of receptor neurons caused by hair stimulation and the mutual inhibition observed by Eckert are being examined, as are the conditions under which reflex stimulation of the extensor muscles occurs.

R. W. Henry

References

1. C. A. G. Wiersma, E. Furshpan, and E. Florey, "Physiological and Pharmacological Observations on Muscle Receptor Organs of the Crayfish, Cambarus clarkii Girard," J. Exptl. Biol. 30, 136 (1953).
2. R. O. Eckert, "Reflex Relationships of Abdominal Stretch Receptors of Crayfish I. Feedback Inhibition of the Receptors," J. Cell. Comp. Physiol. 57, 149 (1961).
3. H. P. Wolverkamp and T. H. Waterman, in The Physiology of Crustacea, Vol. I., edited by T. H. Waterman (Academic Press, Inc., New York, 1960).

C. CUMULATIVE BEHAVIOR OF AVERAGED POTENTIALS

It is quite apparent that data recorded from a living system cannot be considered as a stationary process,[1,2] yet time averages are regularly computed for such data. This lack of stationarity has no effect on the mechanics of forming an average, but it must considerably alter the interpretation of an average. One assumes that the probability distribution of the set of data does not change throughout the entire interval needed to obtain the average. This assumption of stationarity is basic to any interpretation of an average, for it says that data collected during any subinterval of the sample would be the same (statistically speaking) as data collected in some other subinterval. The question of the validity of the average as being characteristic of each individual response must be answered by a close examination of the temporal inhomogeneities that are found in the data themselves.

The averaged evoked response can be defined as an ordered set of averages $\{M_n(t_k)\}_k$, where $M_n(t_k) = \frac{1}{n} \sum_{i=1}^{n} x(T_i+t_k)$, with

$x(t)$ = the instantaneous value of the data

n = number of responses

T_i = instant of time of occurrence of the i^{th} stimulus

t_k = time interval following delivery of the i^{th} stimulus.

In determining the set of averages, $\{M_n(t_k)\}_k$, most algorithms involve the determinations of sums $Y_k = \sum_{i=1}^{n} x(T_i+t_k)$, which can be defined as the cumulative evoked response. These sums are related to the average by a multiplicative scale factor. If $\{x(T_i+t_k)\}_i$ comes from a population with mean μ_{kx} (which itself is not necessarily invariant with

time) and standard deviation σ_{kx}, then the statistic will have mean $\mu_{ky} = n\mu_{kx}$ and standard deviation $\sigma_{ky} = \sqrt{n}\,\sigma_{kx}$. If we plot the statistic Y_k against n, we expect the points to be clustered about a straight line with slope μ_{kx} bounded by confidence limits proportional to $\sqrt{n}\,\sigma_{kx}$. Notice that the standard deviation of this statistic Y_k increases only as $\sqrt{n}$, while the statistic itself increases as n. If μ_{kx} should change once during the interval (T_o+t_k, T_n+t_k) to some new value μ'_{kx}, we expect that data to be clustered about some new straight line having slope μ'_{kx}, and that it will exceed confidence limits based on μ_{kx} and σ_{kx}, if we take a sufficiently large sample after the change. One could thus test the hypothesis that the data are stationary by observing the extent of fluctuations of Y_k, the cumulative evoked response. The key point is that averages based on stationary data build up uniformly – each point Y_k tends to be a straight line. The human observer is rather good at detecting orderliness or trends in a visual presentation of data[3-5]; hence a visual display has been developed which allows the cumulative behavior of a forming average to be examined and subjectively evaluated.

The cumulative response surface (Cum Surface) is a visual display that is designed to allow the examination of the temporal inhomegeneities by observing the formation of an average. Figure XVIII-2 illustrates the formation of this display. A set of accumulating

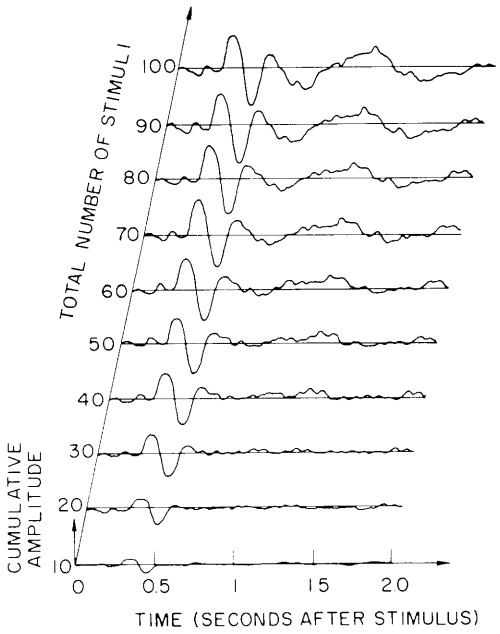

Fig. XVIII-2.

Formation of cumulative response surface. The figure is based on a contiguous sequence of 100 evoked potentials. The first waveform is the sum of the first 10 responses, the second is the sum of the first 20 responses including the 10 contributing to the first waveform, and so forth. Each succeeding waveform is displaced up and to the right of its predecessor.

(partial) sums, $\{Y_k\}_k = \left\{ \sum_{i=1}^{n} x(T_i+t_k) \right\}_k$, are displayed successively. The first sum is based on M evoked potentials (n=M). The second set, which is displaced up and to the right, contains the first M potentials plus M additional potentials (n=M+M). The N^{th} waveform is

the sum of NM potentials and includes the (N-1)M potentials contained in the immediately preceding waveform (n=MN). In this example M = 10, N = 10. The intensity of the oscilloscope beam is modulated according to the displayed accumulating sum.

An example of the cumulative response surface is presented in Fig. XVIII-3. The data

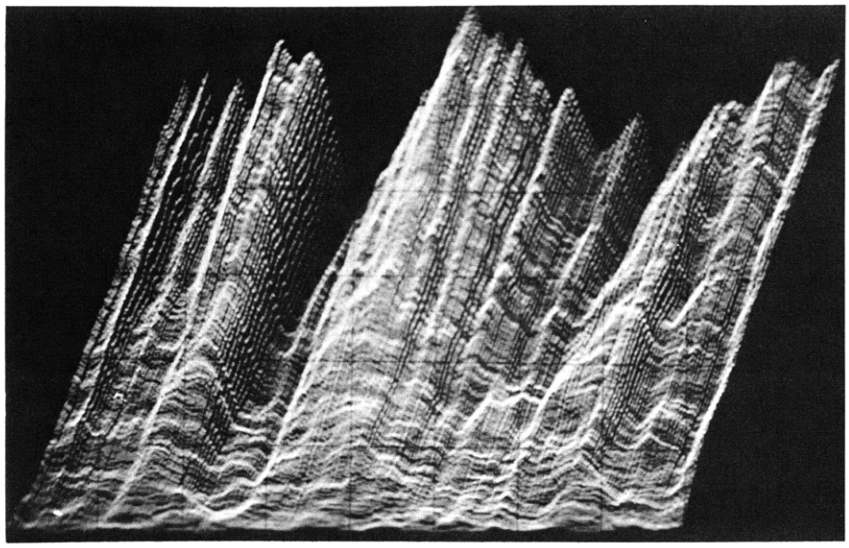

Fig. XVIII-3. Single cumulative response surface based on data recorded from a sleeping human subject. The figure is formed from a sequence of 256 accumulating averages covering approximately 11 minutes. Each average covers 2 sec starting 50 msec before the stimulus is presented. This figure includes the end of an REM stage and the beginning of stage II sleep. The evolution of late components in the average may be readily observed. The data are clearly nonstationary and thus the interpretation of the average is difficult. Data from vertex-midline occipital electrode pair recorded on night 8, subject R.S. Stimulus was a 50-dB SL click presented once each 2.5 sec.

used in forming this surface were recorded from the scalp of a sleeping human subject; included are recordings from the end of a period of Rapid Eye Movement (REM), sleep, and the beginning of stage II sleep. The evolution of late components in the average is clearly visible. The resulting average, based on 256 evoked potentials, is very difficult to interpret, since it is obviously based on nonstationary data. The display suggests that an average based on potentials 100 to 256 might be more representative of individual responses. Twelve cumulative response surfaces are shown in Fig. XVIII-4. A plot of the final value of each accumulating sum is displayed at the right of the corresponding surface. If the data were stationary, then the surface should develop uniformly. It is quite apparent that this is not the case in the interval needed to accumulate 256 responses, even though the classification of the EEG in terms of stage-of-sleep

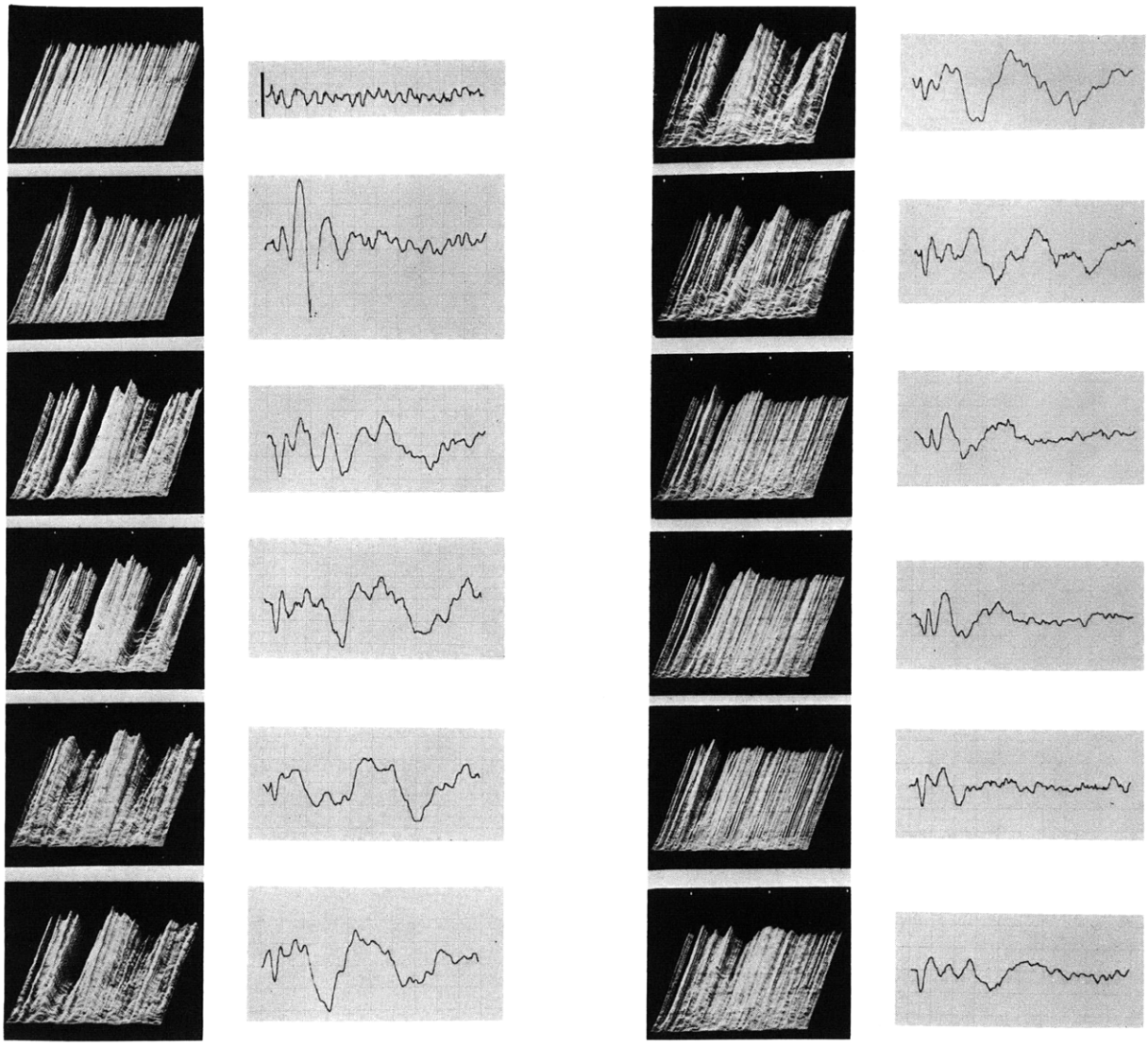

Fig. XVIII-4. Sequence of 12 cumulative response surfaces based on data recorded from a sleeping human subject. The surface illustrated in Fig. XVIII-3 is the top surface in the right-hand column in this figure. A plot of the final value of each accumulating sum is displayed to the right of the corresponding surface. Data from vertex-midline occipital electrode pair recorded on night 8, subject R.S. Stimulus was 50 dB SL acoustic click presented once each 2.5 sec. Each average covers 2 sec and starts 50 msec before the stimulus presentation. The vertical bar in the left corner average represents 20 μV.

remains unchanged.

The cumulative response surface is a three-dimensional display. The cumulative behavior of the evoked potential at a particular time, t_k, after the stimulus presentation appears as the intersection of the surface with a plane of constant latency (constant k for a discrete analysis). This two-dimensional display of $\{Y_k\}_n$ allows a careful examination of the cumulative evoked response at any selected time. It has been usefully applied to analyzing data recorded from the brains of behaving animals,[6, 1, 2] as well as data recorded from sleeping human subjects. Figure XVIII-5 shows the cumulative evoked response at 50 msec, $Y_{-50} = \sum_{i=1}^{n} x(T_i - 50 \text{ msec})$, before the stimulus presentation and at 250 msec, $Y_{+250} = \sum_{i=1}^{n} x(T + 250 \text{ msec})$, after the stimulus presentation as a function of n, the sample size. The upper trace corresponds to a positive peak in the time-locked

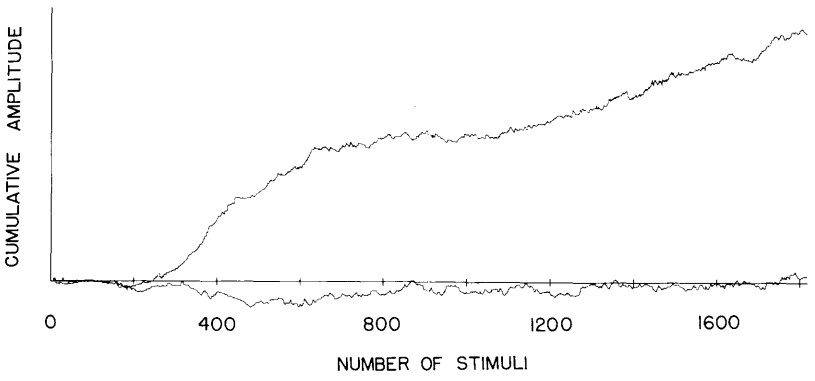

Fig. XVIII-5. Cumulative evoked responses (Cum) based on the evoked response 50 msec before and 250 msec after the stimulus delivery. These plots represent the intersection of a plane of constant latency with the cumulative response surface. The data correspond to that illustrated in the first seven surfaces shown in Fig. XVIII-4.

activity following the stimulus delivery. The lower trace refers to the cumulative behavior of the neuroelectric potential before the stimulus is presented. The expected values of these traces are, of course, straight lines having constant slope if the data are stationary. The lower line can be used as a sort of qualitative control to judge the deviation from the expected value of the upper trace, because of the large standard deviation of the data. In the approximately 75-minute interval that is included it seems that the mean of the data at 250 msec after stimulus presentation would be better characterized by 4 different values rather than by a single number.

It should be pointed out that this display can be produced without particularly elaborate equipment if the signal averager is capable of displaying an accumulating sum.

All that one needs is an oscilloscope with z-axis modulation (Tektronix 536, or a modified Tektronix 561A) and a slowly increasing voltage that can be added to the output display of the averager so as to provide the perspective. The averages presented in the accompanying figures were computed on ARC.[7] Prof. S. L. Chorover of the Department of Psychology, M.I.T., suggested that a Technical Measurements Corporation Computer of Average Transients (CAT) could be used to produce the display by alternately adding a response and then subtracting a constant that is slightly smaller than the constant normally added by the analog-to-digital conversion process within the CAT.

S. K. Burns

References

1. R. Melzack and S. K. Burns, "Neuropsychological Effects of Early Sensory Restriction," Boletin del Instituto de Estudios Medicos y Biologicos 21, 407-425 (1963).
2. R. Melzack and S. K. Burns, "Neurophysiological Effects of Early Sensory Restriction," Exptl. Neurol. 13, 163-175 (1965).
3. P. M. McGregor, "A Note of Trace-to-Trace Correlation in Visual Displays: Elementary Pattern Recognition," J. Brit. IRE 15, 329-331 (1955).
4. M. I. Skolnik and D. G. Tucker, "Discussion on Detection of Pulse Signals in Visual Displays," J. Brit. IRE 17, 705-706 (1957).
5. D. G. Tucker, "Detection of Pulse Signals in Noise: Trace-to-Trace Correlation in Visual Displays," J. Brit. IRE 17, 319-329 (1957).
6. S. K. Burns, "Display of the Cumulative Behavior of Evoked Responses," Quarterly Progress Report No. 78, Research Laboratory of Electronics, M.I.T., July 15, 1965, pp. 260-263.
7. W. A. Clark, R. M. Brown, M. H. Goldstein, Jr., C. E. Molnar, D. F. O'Brien, and H. E. Zieman, "The Average Response Computer (ARC): A Digital Device for Computing Averages and Amplitude and Time Histograms of Electrophysiological Responses," IRE Trans., Vol. BME-8, pp. 46-51, 1961.

D. HYBRID SIMULATION OF HODGKIN-HUXLEY MODEL FOR NERVE MEMBRANE

A computer simulation of the Hodgkin-Huxley model for nerve membrane was developed on a hybrid (analog and digital) facility. [The Beckman-Scientific Data System Hybrid Computer was made available to the author by the Instrumentation Laboratory, M.I.T.] The results from the simulation were compared with the original calculations of Hodgkin and Huxley.[1] Also, data predicted by the simulation were compared with more recent experimental results.

In 1952, A. L. Hodgkin and A. F. Huxley presented an empirical model in which the current-voltage relations of a section of nerve membrane with uniform potential (space-clamped) can be represented by the network shown in Fig. XVIII-6.

E_m is the potential across the membrane. E_{mo} is the value of this potential in the resting state, that is, the state in which none of the model parameters are varying with time. The sum of the current density charging the capacitance, C_m, and the ionic current densities flowing through the parallel conductances is the total membrane current

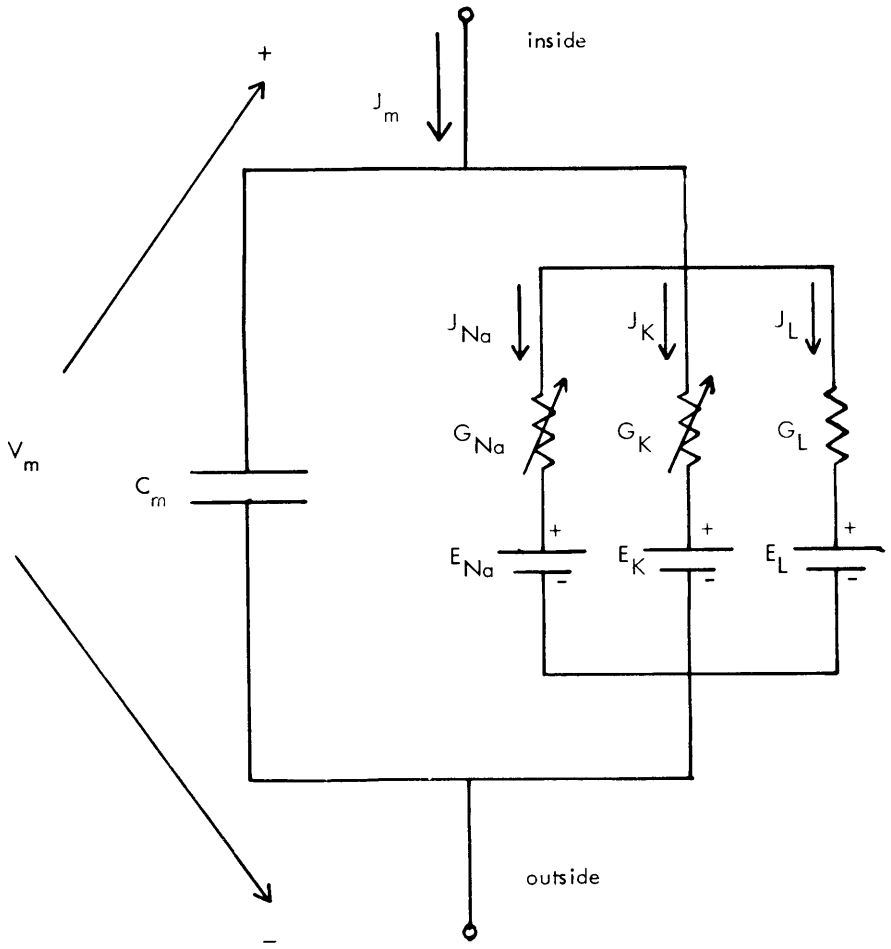

$G_{Na} = \bar{G}_{Na} m^3(E_m,t)h(E_m,t)$

$\bar{G}_{Na} = 120$ mmhos/cm^2

$G_K = \bar{G}_K n^4(E_m,t)$

$\bar{G}_K = 36$ mmhos/cm^2

$\bar{G}_L = 0.3$ mmhos/cm^2

$E_{Na} = 55$ mvolts

$E_K = -72$ mvolts

$E_L = -50$ mvolts

$E_{mo} = -60$ mvolts

$C_m = 1.0$ microfarad/cm^2

Fig. XVIII-6. Electrical network representing nerve membrane.

density, J_m The ionic current density has three components, each of which is determined by a potential difference and a conductance. For example, J_{Na}, which represents the flow of sodium ions through the membrane, is equal to the product of the sodium conductance, G_{Na}, and the potential difference $(E_m - E_{Na})$. Similarly, J_k is equal to G_k

times (E_m-E_k). The product of G_L and (E_m-E_L) represents current density attributable to the flow of chloride and other ions through the membrane.

The important characteristics of the membrane are determined by the sodium and potassium conductances. These are functions of membrane potential, E_m, and time, while all other parameters of the network are constant.

The batteries, E_{Na} and E_k, represent the potential arising from the differences in concentrations of the respective ions inside and outside of the membrane. The values of these batteries are the Nernst equilibrium potentials for the respective ions. The value E_L is approximately equal to the Nernst equilibrium potential for chloride ions. Its exact value is, however, such that the total ionic current is zero at the resting potential. The resting potential is -60 mV when the network is not excited by external currents or voltages.

The parameters of the model were chosen to fit the voltage clamp data of the giant axon of the squid, that is, the data used were the membrane current records resulting from changes in the externally constrained membrane potential. The model predicts, however, the electrical behavior of the axon membrane for a variety of experimental conditions for which the membrane potential is not so constrained.

For ease of calculation, the value of the resting potential was subtracted from all potential variables

$$V_m = E_m - E_{mo} \qquad V_k = E_k - E_{mo}$$

$$V_{Na} = E_{Na} - E_{mo} \qquad V_L = E_L - E_{mo}$$

Thus, $V_m = 0$ when the membrane is at rest.

Hodgkin and Huxley chose to fit the conductances by the following variables: $G_k = \overline{G}_k n^4(V_m,t)$, $G_{Na} = \overline{G}_{Na} m^3(V_m,t)\, h(V_m,t)$, and $G_L = \overline{G}_L$. The conductance factors, $n(V_m,t)$, $m(V_m,t)$, and $h(V_m,t)$ are solutions to first order, nonlinear, time-variant differential equations; $\overline{G}_k$, $\overline{G}_{Na}$, and $\overline{G}_L$ are constant.

Thus the total membrane current as a function of membrane potential and time is

$$J_m = C_m(dV_m/dt) + \overline{G}_k n^4(V_m,t)(V_m-V_k)$$

$$+ \overline{G}_{Na} m^3(V_m,t)\, h(V_m,t)(V_m-V_{Na}) + \overline{G}_L(V_m-V_L).$$

Current density is in units of $\mu A/cm^2$; potential, mV; conductance, $mmho/cm^2$; capacitance, $\mu F/cm^2$; and time, msec. The parameters of the equation above are defined below for a temperature of 6.3°C.

$$\frac{d}{dt}[n(V_m,t)] = \alpha_n(V_m)[1-n(V_m,t)] - \beta_n(V_m)\, n(V_m,t)$$

$$\frac{d}{dt}[m(V_m,t)] = \alpha_m(V_m)[1-m(V_m,t)] - \beta_m(V_m)\, m(V_m,t)$$

$$\frac{d}{dt}[h(V_m,t)] = \alpha_h(V_m)[1-h(V_m,t)] - \beta_h(V_m)\, h(V_m,t)$$

$$\alpha_n(V_m) = 0.01(V_m+10)/(\exp[(V_m+10)/10]-1)$$

$$\beta_n(V_m) = 0.125\, \exp[V_m/80]$$

$$\alpha_m(V_m) = 0.1(V_m+25)/(\exp[(V_m+25)/10]-1)$$

$$\beta_m(V_m) = 4\, \exp[V_m/18]$$

$$\alpha_h(V_m) = 0.07\, \exp[V_m/20]$$

$$\beta_h(V_m) = 1.0/(\exp[(V_m+30)/10]+1)$$

$\overline{G}_K = 36$ mmhos/cm^2 $\qquad$ $\overline{G}_{Na} = 120$ mmhos/cm^2

$G_L = 0.3$ mmhos/cm^2 $\qquad$ $V_K = -12$ mV

$V_{Na} = 115$ mV $\qquad$ $V_L = 10.063$ mV

$$C_m = 1.0\ \mu\text{F/cm}^2.$$

A complete block diagram of the hybrid simulation of the Hodgkin-Huxley equations is shown in Fig. XVIII-7. All variables – potentials, currents, and conductances – were represented by voltages that were scaled by appropriate factors. The time scale of the solution was altered by changing the gains of all of the integrators of the system. The values of the 6 rate constants, α_n, β_n, α_m, β_m, α_h, and β_h, were calculated and stored in the memory of the digital computer. The digital computer sampled the analog membrane potential and determined the appropriate set of 6 rate constants and placed their values on the 6 digital-to-analog output lines. All other computations were done on the analog portion of the hybrid computer.

The following voltage and time scale factors were chosen.

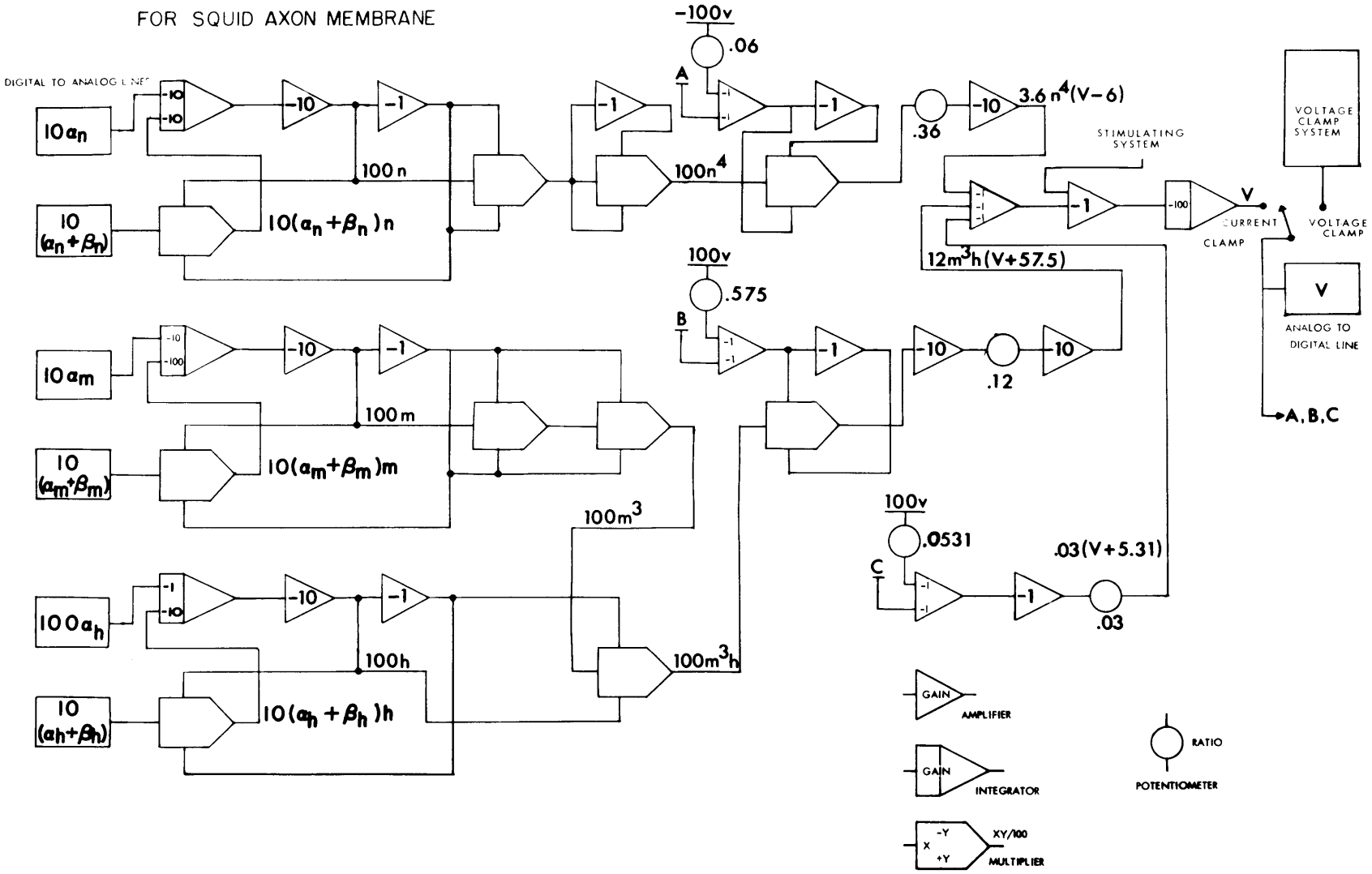

Fig. XVIII-7. Complete hybrid simulation of the Hodgkin-Huxley equations.

Real Variable	Simulation Variable
1.0 mV	-0.5 V
1.0 mmho/cm^2	0.1 V
1.0 μA/cm^2	-0.05 V
1.0 msec	100.0 msec

The simulation operated in two different modes. When the switch in Fig. XVIII-7 is set in the current clamp position, the simulation represents a space-clamped section of axonal membrane. When an adequate stimulus is applied, the simulated membrane potential exhibits a membrane action potential. A voltage-clamped section of axon membrane is represented by the simulation when the switch is set in the voltage-clamp position. The membrane potential may be changed to any desired value and the resulting ionic current can be recorded.

Typical voltage clamp records from the simulation are shown in Fig. XVIII-8. The membrane potential here was depolarized with a 60-mV pulse.

The response of the simulated space-clamped membrane to a short current pulse is shown in Fig. XVIII-9. Along with the time course of the membrane action potential is shown the time course of ionic current density, the sodium, potassium, and leakage current densities, $n(V_m,t)$, $m(V_m,t)$, and $h(V_m,t)$.

Detailed comparisons with the solutions that were calculated by Hodgkin and Huxley showed that the hybrid simulation reproduced the solutions accurately. The following phenomena have been investigated.

1. Time course of ionic current densities under voltage clamp constraints.
2. Time course membrane action potential.
3. Time course of membrane impedance during an action potential.
4. Existence of threshold and the form of the strength-duration curve.
5. Time course of subthreshold response.
6. Existence of refractoriness.
7. The properties of repetitive activity under prolonged depolarization.
8. Form of action potential from anode break excitation.

Furthermore, the predictions of the model were compared with results from experiments in which the internal and external ionic concentrations of potassium and sodium were varied (see Baker, Hodgkin and Shaw[2]). The results of replacing internal and external potassium with sodium are shown in Fig. XVIII-10. It was found that for experimental conditions in which the external solution has a composition close to normal, the Hodgkin-Huxley equations predict resting potential changes that agree fairly accurately with experimental results. Under these

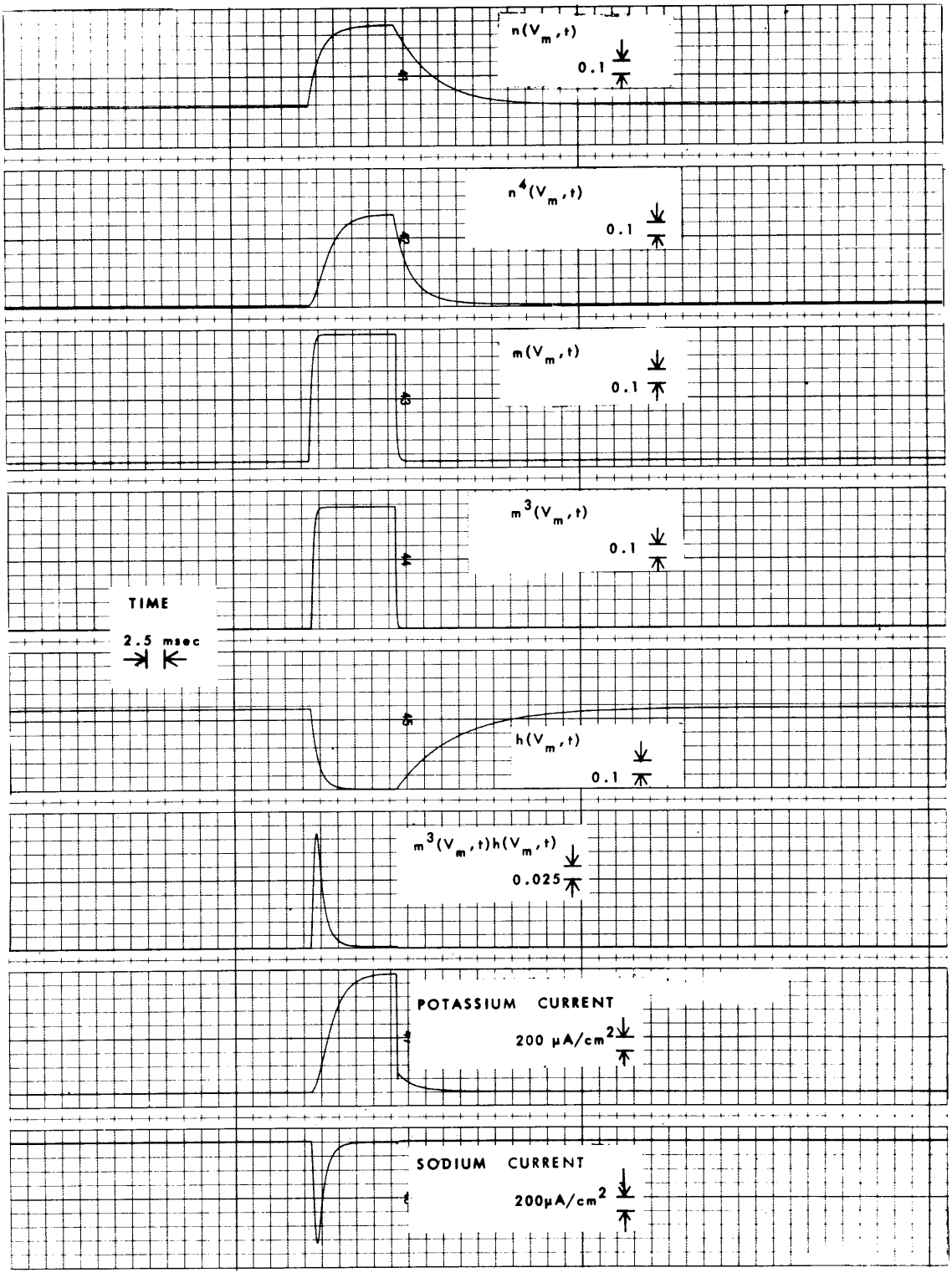

Fig. XVIII-8. Simultaneous time course of $n(V_m,t)$, $n^4(V_m,t)$, $m(V_m,t)$, $m^3(V_m,t)$, $h(V_m,t)$, $m^3(V_m,t)\,h(V_m,t)$, $J_k(V_m,t)$, and $J_{Na}(V_m,t)$ for a 60-mV pulse of 12.5-msec duration under voltage clamp.

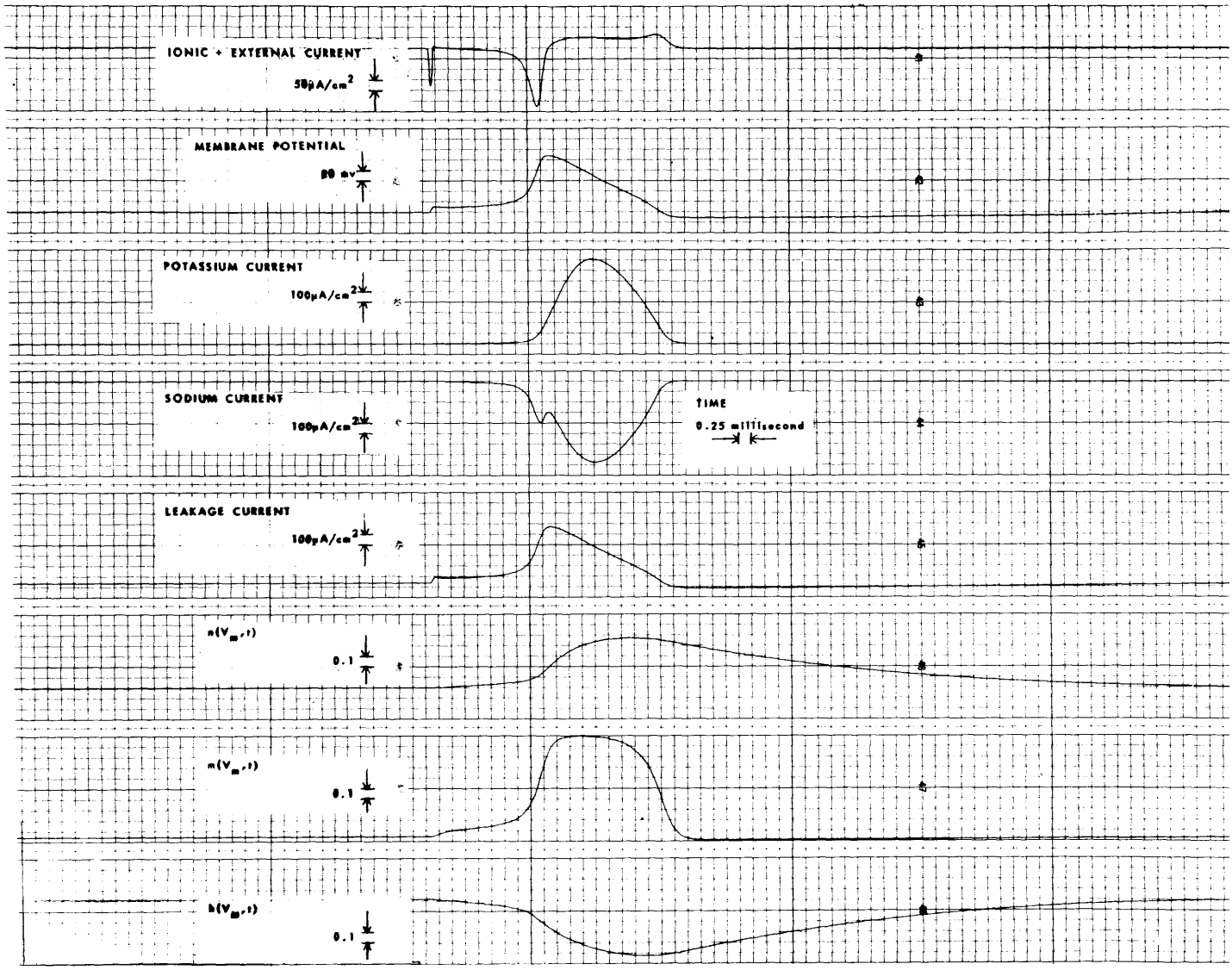

VIII-9. Simultaneous time course of $J_{ionic}(V_m, t)$, $V_m(t)$, $J_k(V_m, t)$, $J_{Na}(V_m, t)$, $J_L(V_m, t)$, $n(V_m, t)$, m $h(V_m, t)$ for a membrane action potential. The stimulus is an external current density, 85 amplitude, and 0.5 msec in duration.

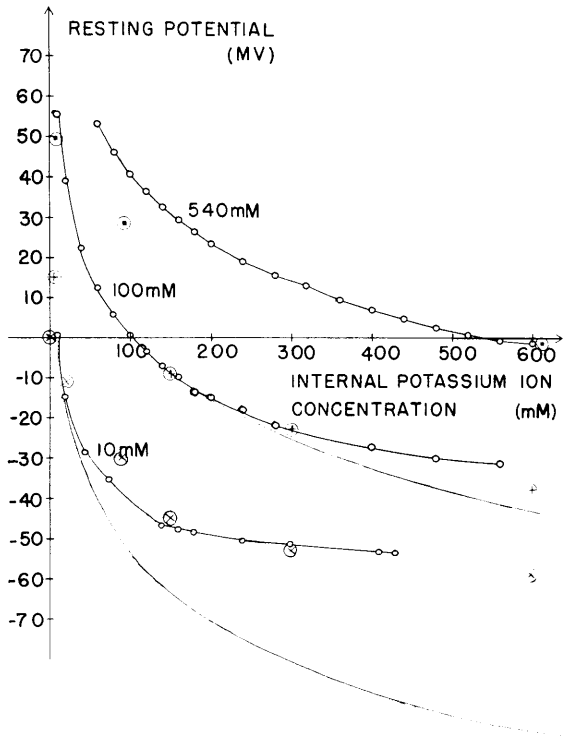

Fig. XVIII-10. Simulated resting potential vs internal potassium ion concentration for three external potassium ion concentrations. Empty circles represent recordings from the hybrid simulation. A curve was drawn through the points by the author. The circled marks are from Baker, Hodgkin, and Shaw, 1962. They represent the average of many experimental points. The lines are drawn according to the appropriate Nernst potassium equilibrium potential. The Nernst potential is not visible in the upper curve because it coincides with the experimental curve.

conditions, the H-H equations fit experimental data at least as well as other models that have been proposed for the resting potential.[2-4]

A full report of this study appears in the author's Master's thesis.

P. Demko, Jr.

References

1. A. L. Hodgkin and A. F. Huxley, "A Quantitative Description of Membrane Current and Its Application to Conduction and Excitation in Nerve," J. Physiol. 117, 500-544 (1952).

2. P. F. Baker, A. L. Hodgkin, and T. I. Shaw, "Replacement of Axoplasm of Giant Nerve Fibers with Artificial Solutions," J. Physiol. 164, 330-354 (1962).

3. A. L. Hodgkin and B. Katz, "The Effect of Sodium Ions on the Electrical Activity of the Giant Axon of the Squid," J. Physiol. 108, 37-77 (1949).

4. T. F. Weiss, "Notes for Course 6.372 – Introduction to Neuroelectric Potentials," Massachusetts Institute of Technology, 1967, see Chap. II.